

SHOCK RADIATION TESTS FOR ICE GIANT ENTRY PROBES INCLUDING CH₄ IN THE T6 FREE-PISTON DRIVEN WIND TUNNEL

Joseph Steer¹, Peter Collen¹, Alex Glenn¹, Christopher Hambidge¹, Luke Doherty¹, Matthew McGilvray¹, Stefan Loehle², and Louis Walpot³

¹*Oxford Thermofluids Institute, University of Oxford, Oxford, UK*

²*High Enthalpy Flow Diagnostics Group (HEFDiG), Institute of Space Systems (IRS), Stuttgart, Germany*

³*ESA/ESTEC, Keplerlaan Noordwijk, The Netherlands*

ABSTRACT

The Ice Giants, Uranus and Neptune, represent a largely unexplored, interstitial class of planetary objects that fit between the Gas Giants and the smaller terrestrial worlds, such as Earth, in terms of their size and elemental composition and are therefore a missing link in our understanding of extrasolar planetary evolution. The scientific potential of a mission to the Ice Giants is well recognised and has been identified by NASA and ESA as a high priority on several occasions, most recently in the 2023 - 2032 Decadal Survey. The payload capacity of such a spacecraft is limited by the requirement for a bulky heat shield, made necessary by the paucity of ground test data for convective and radiative heat flux at proposed entry trajectories. This paper describes an experimental study of shock layer radiation via emission spectroscopy at Ice Giant entry conditions in the T6 free-piston driven wind tunnel. Shock waves of up to 18.9 km s^{-1} were driven through H/He mixtures containing up to 5% CH₄ by mole. The magnitude of spectral radiance at the peak and in the immediate post-shock region appears to be strongly affected by the concentration of CH₄ in the test gas. Thorough cleaning of the shock tube between each test was found to be very important for obtaining high quality data given the relatively low signal levels.

Key words: ice giant; shock layer radiation; high enthalpy.

1. INTRODUCTION

The 2023 - 2032 Decadal Survey has recommended that NASA's highest priority new flagship mission should be a Uranus orbiter and probe with a launch date in the early 2030s [1]. This and previous publications from both NASA and ESA [2, 3] have prompted a resurgence of interest in simulating the heat flux that would be experienced by such a vehicle with a view to increasing the available payload margin. Heat flux may be separated into a convective component, due to the

Table 1: Tropospheric composition of the Ice Giants by volume from [6]

Species	Uranus	Neptune
He	15.2%	14.9%
CH ₄	1.4 - 4%	2 - 5%
NH ₃	30 - 90 ppm	40 - 200 ppm
H ₂ O	<5%	27%
PH ₃	<2 ppm	<1.1 ppb at 0.7 bar
H ₂ S	0.4 - 0.8 ppm	1 - 3 ppm

movement of hot shock-layer gas over the surface of the vehicle, and a radiative component, due to the excitation and subsequent re-emission of energy by atoms in the shock-layer. Uncertainties in predictive models for the heat flux magnitude were evaluated through Monte Carlo analysis at NASA Ames [4] and it was found that for Uranus entry trajectories the velocities and shock-layer temperatures were low enough that radiative heating is negligible. Tests in NASA EAST facility confirmed this finding, observing no shock-layer radiation below 25 km/s in an 89%H₂/11%He mixture [5].

Although significant progress in Gas Giant entry research has been made in the last ten years, many studies have neglected the influence of trace components such as CH₄ on the aeroheating environment. In a review paper, [6] summarises the observed abundance of tropospheric and stratospheric constituents on the Ice Giants. These values are reproduced in Tables 1 and 2.

To date, there have been no direct measurements of the effect of CH₄ on radiative heat flux for Ice Giant trajectories. Recent simulations from [7] indicate that the presence of 1.5% CH₄ will have a significant effect on the radiative heating environment for entry speeds as low as 18 km/s where previously it was thought that no significant radiation would be present until 25 km/s or greater. The bulk of the deceleration and therefore aeroheating for Ice Giant trajectories is expected to occur in the stratosphere [2], where CH₄ abundance on Neptune is expected to be an order of magnitude

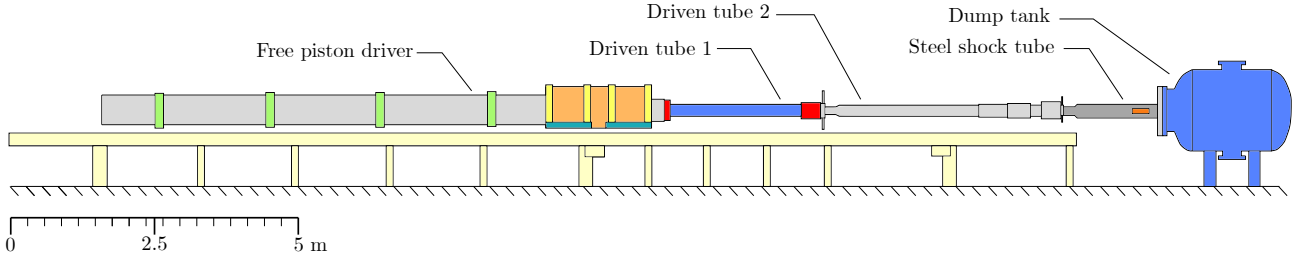


Figure 1: Schematic of the T6 facility in shock tube mode, showing the arrangement of different components. The 'steel shock tube' has been designed specifically for Ice Giant radiation measurements.

Table 2: Stratospheric composition of the Ice Giants by volume from [6]

Species	Uranus	Neptune
CH ₄	16 ppm at 50 mbar	0.115% at 5 mbar
C ₂ H ₂	0.25 ppm at 0.2 mbar	0.033 ppm at 0.5 mbar
C ₂ H ₄	$<2 \times 10^{-14}$ at 10 mbar	0.8 ppb at 0.2 mbar
C ₂ H ₆	0.13 ppm at 0.2 mbar	0.85 ppm at 0.3 mbar
C ₃ H ₄	0.36 ppb at 0.4 mbar	0.12 ppb at 0.1 mbar
C ₄ H ₂	0.13 ppb at 0.4 mbar	0.003 ppb at 0.1 mbar
CO ₂	0.08 ppb at 0.14 mbar	0.78 ppm at 0.1 mbar
CO	6 ppb at 0.5 mbar	1.1 ppm at 0.1 mbar
H ₂ O	3.8 ppb at 0.03 mbar	2.5 ppm at 0.16 mbar
D/H	4.4×10^{-5}	4.1×10^{-5}

lower than the value modelled by Coelho - abundance on Uranus is expected to be three orders of magnitude lower. Given that the Decadal Survey has identified a Uranus mission as the priority the requirement for detailed studies of surface heat flux with CH₄ mixtures is lessened. However, establishing this capability will still be informative for modelling of the atmosphere and heat shield recession post-flight as done by, for example, [8].

2. FACILITY DESCRIPTION

T6, as shown in Figure 1, is a multi-mode hypersonic wind tunnel. The free-piston driver, which generates pressures on the order of 50 MPa during a shot, may be coupled to a range of downstream components to allow operation of the facility as either a shock tube, expansion tube, expansion tunnel, or reflected shock tunnel. T6 is the only operational expansion tube/shock tube facility in Europe. In the present work, Ice Giant experiments will be run in shock tube mode to provide insight into the non-equilibrium thermochemistry occurring in the shock layer. A more detailed overview of T6 can and experiments run to date can be found in [9].

Shock tubes are ubiquitous in fundamental fluid dynamics research because of their simplicity and versatility. Shock tubes are currently the best source of measurements of shock layer radiation, which can constitute a

significant fraction of the total heat flux into an entry vehicle. Recent experiments by [5] have shown that at the entry conditions of interest for the Ice Giant entry the radiative component of total heat flux to the front surface of the vehicle will be minimal, only becoming significant for higher speed Saturn trajectories. However, it could still be highly informative for the investigation of the chemical kinetics, non-Boltzmann behaviour, the extent of the non-equilibrium region.

3. EXPERIMENTAL ARRANGEMENT

In the present work, a new steel shock tube featuring two 190 x 10 mm windows has been designed to facilitate study of the shock layer at Ice Giant entry conditions via spectroscopy. The tube incorporates 8 axial locations to mount shock timing stations, which at 5 locations feature holes on both sides of the tube. The tube also features a tertiary diaphragm station so that the driven tube volume can be isolated from the dump tank volume, allowing higher vacuums to be achieved and minimising the quantity of hydrogen required to reach a given test pressure. This has successfully been fitted to the existing infrastructure and passed hydraulic testing at 175 bar. Further details of this and other recent upgrades are included in [10].

The tube features a large port just downstream of the measurement windows to allow connection to a turbomolecular pump with minimal pumping resistance. With this arrangement an ultimate vacuum of less than 1 mPa was achieved with a leak rate of less than 1 mPa s⁻¹. Delivery of the hydrogen/helium test gas was achieved via a sample cylinder system designed and implemented specifically for this work. A sample cylinder of variable volume (300 - 5000 cc) was evacuated and pressurised to 1 - 3 bar with the test gas while isolated from the driven tubes. Just before the test, the contents of the sample cylinder were introduced to the evacuated driven tubes and allowed to equalize in pressure via a nearly ideal process ($p_1 V_1 = p_2 V_2$) where the test pressure was measured on a low range gauge. With practise this method was found to be a repeatable and accurate way to deliver the test gas.

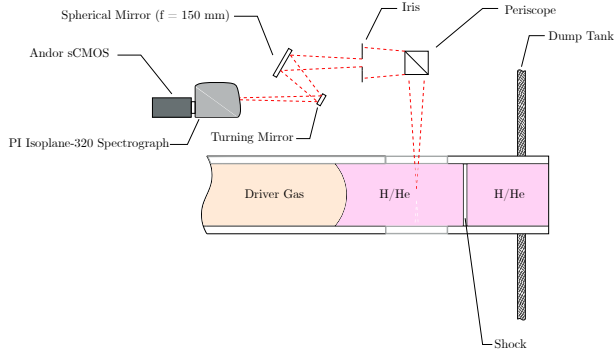


Figure 2: Schematic diagram of the experimental setup planned for use in shock tube mode, reproduced from [11]

Emissions from the radiating shock layer are recorded via a PI Isoplane-320 Spectrograph coupled to an Andor iStar-sCMOS. The measurement window used was UV grade fused silica from Crystran Ltd, a black coloured blank was installed on the opposite side of the tunnel to minimise the impact of reflections on the data. Before each test a spatial, intensity, and wavelength calibration of optical setup were performed. Spatial calibration of the spectrometer was achieved with the aid of a custom alignment plate. The plate was designed to bolt onto the opposite side of the tube and had holes drilled along the centreline of the tunnel with a positional tolerance of 0.05 mm. By lighting the back side of this plate with a diffuse light source the holes were clearly visible in the sCMOS view as near points. These points were then used as reference to set the desired field of view of the spectrometer via fine adjustment of optical mirrors. Intensity calibration of the spectrometer was achieved via the use of an integrated light source. The model used was a Bentham SRS8 Integrating Sphere. During the calibration process, the integrated light source was fixed to the opposite side of the tube and positioned in the line of sight of the spectrometer. A series of images were then collected using the 'accumulate' feature on the Andor camera, each image having the same exposure time and gain settings as the test exposure. The same process was then completed with the integrated light source off which provided a reference background image. Wavelength calibration was completed using a Princeton Instruments IntelliCal Hg and Ne/Ar laser. The calibration and post-processing techniques used have been described in detail by Collen [11] and Glenn [12]. A schematic diagram of the experimental setup used is shown in Figure 2.

The Andor camera was triggered using a micro-controller based delay generator. The controller monitors the pressure signals at two locations close to the end of the shock tube and then predicts the time of arrival of the shock at the window. As a compromise between signal to noise ratio and spatial resolution, a camera exposure time of 500 ns was used for all experiments. The spectrometer was focused either in the 'UV' (330 - 550 nm) or in the 'red' (440 - 680 nm). Spatial radiance profiles obtained for each condition are shown in Figure 6. For all tests the

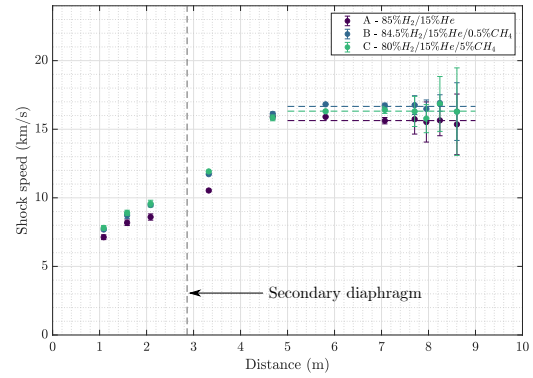


Figure 3: Shock speed profiles for tested conditions

test gas slug length was approximately 40 mm. This was evidenced by a large increase in radiance from helium species, indicating arrival of the driver gas.

4. TESTED CONDITIONS

4.1. Condition Details

Conditions for nominal composition (85% H_2 /15% He) and nominal composition with methane (0.5% and 5% CH_4) gas mixtures have been developed and are detailed in Table 3. In order to achieve the high shock speeds required for Ice Giant entry, a pure helium secondary driver was utilised in all tests. The secondary driver and test gas fill pressures, psd_1 and p_1 respectively, were selected in order to maximise the achievable shock speed. The primary and secondary shock speeds, U_{s1} and $U_{s2/\infty}$ respectively, were calculated using measurements from shock timing stations distributed along the length of the facility.

Figure 3 shows the measured shock speeds for each condition. Moderate shock deceleration was observed in most tests. For example, the shock speed in shot 372 peaked at 18.4 km s^{-1} but decelerated to 17.0 km s^{-1} by the time it reached the observation window. Shock speed uncertainties were calculated using the method detailed by [13] and as such are much higher near the observation window due to the decreased sensor spacing. The peak shock speed seen in the campaign for 18.9 km s^{-1} in T6s365 for condition B where the fill pressure was 0.1 torr.

Figure 4 shows a comparison of the achieved experimental performance versus several candidate Ice Giant entry trajectories proposed by ESA [2]. Similarity between facility and flight is obtained along the stagnation line when freestream velocity and density are matched. For a given pressure, the temperature in the lab is typically

Table 3: Summary of conditions tested in shock tube mode

Condition	Test Gas Composition [%v/v]	psd_1 [Pa]	p_1 [Pa]	U_{s1} [km/s]	U_{s2} [km/s]	Mirels Slug Length [mm]	Mirels Test Time [μ s]
A	85% H_2 /15%He	1000	12.9	8.8	16.7	38	2.3
B	84.5% H_2 /15%He/0.5% CH_4	1000	12.8	8.8	16.4	39	2.4
C	80% H_2 /15%He/5% CH_4	1000	13.0	8.8	16.3	41	2.5

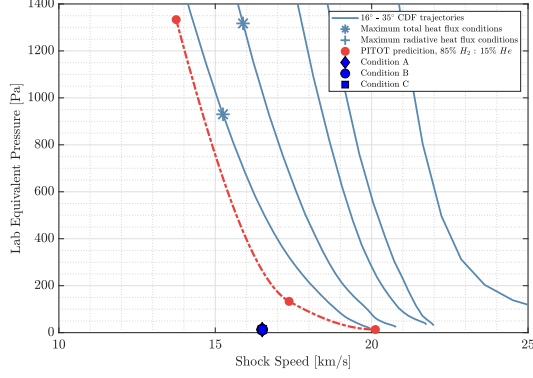


Figure 4: Plot of achieved performance versus candidate ESA trajectories and PITOT predictions

higher than what would be encountered in flight and therefore the atmospheric density is converted to an equivalent pressure at laboratory conditions, which is what is shown in Figure 4. Fully theoretical PITOT predictions for the existing 'high' driver condition of 46.2 MPa, a secondary driver fill of 1 kPa pure helium, and test gas fill pressures of 0.1, 1, and 10 torr are also included. Options for improving the facility performance include reducing the diaphragm opening time which would necessitate a different diaphragm material. Design of a more powerful driver condition is also possible, but would require manufacture of a lighter piston.

4.2. Pressure Traces

Figure 5 shows static pressure traces obtained at the observation window. CEA predicts post-shock pressures of 3.1, 3.3, and 4.1 kPa for conditions A, B, and C respectively if the average shock speed over the last five shock timing stations is used as the input. This is broadly consistent with the values in Figure 5 and minor discrepancies are resolved by using the local shock speed as the input.

4.3. Spatial Radiance Profiles

Figure 6 shows the spatial distribution of spectral radiance obtained for the three conditions. The data are characterised by a non-equilibrium peak at the shock

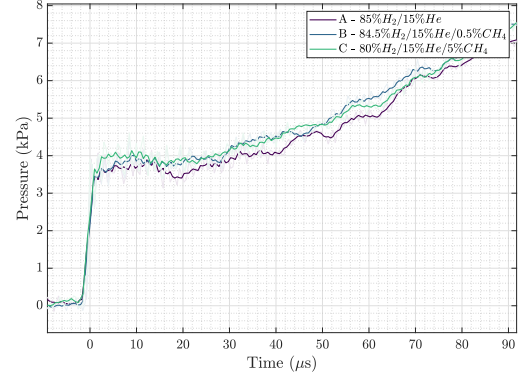


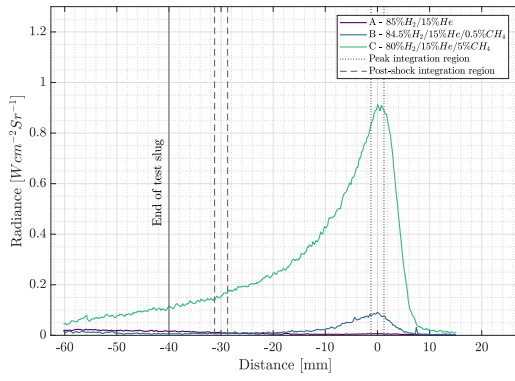
Figure 5: Plot of wall pressure traces at the observation window for tested conditions

front and subsequent relaxation toward equilibrium. The magnitude of spectral radiance at the peak and in the immediate post-shock region appears to be strongly affected by the concentration of CH_4 in the test gas - the maximum spectral radiance at the peak increases by approximately an order of magnitude for each increase in CH_4 concentration. It is unclear to what extent equilibrium is reached in any of the conditions, particularly the 5% CH_4 case.

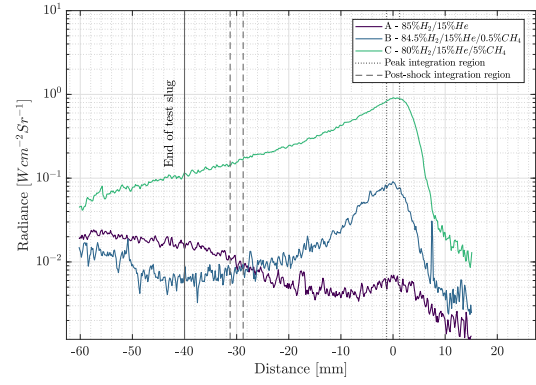
In the initial series of experiments significant precursor effects are evident, indicating that the light emitted ahead of the shock wave has been reflected by the shock tube walls has been erroneously captured by the spectrometer and superimposed on the data as has been discussed by [12]. Another contributor to these effects could be spatial smearing caused by overexposure of the camera during the test time. The camera exposure time was initially kept constant at 500 ns, during which time the shock front would move 7.5 mm if travelling at a speed of 15 km s^{-1} . These effects were largely removed by 'blacking out' the side of the tunnel opposite the camera to absorb possible reflections and halving the camera gating time to 250 ns.

4.4. Wavelength Radiance Profiles

Figures 7, 8, and 9 shows radiance obtained versus wavelength for the 0%, 0.5%, and 5% CH_4 conditions respectively. Two profiles are presented, one corresponding to the peak region ($\pm 1 \text{ mm}$) and one corresponding to the end of the test slug (30 mm behind the peak \pm



(a) Linear scale



(b) Log scale

Figure 6: Spatial radiance profiles obtained for tested conditions

1 mm). In keeping with the findings of Cruden et al. [5] negligible radiance was observed for the 0% CH₄ mixture, evidence of the H- β line at 486 nm is notably absent. What radiation is present is likely from residual carbonaceous species as the profile seems to correspond to the Deslandres-D'Azambuja band system of C2 and CH.

5. FUTURE WORK

5.1. Comparison to Numerical Simulations

Park et al. [14, 15] have developed and validated theoretical models to describe the thermochemical nonequilibrium and radiation phenomena in the shock layer for hydrogen/helium mixtures against the work of [16, 17]. Park has also developed a model that accounts for CH₄ [18] but expressed a desire for experimental data against which to validate it [19]. The experiment described would produce a 30 km s⁻¹ shockwave in a 1 torr mixture 80% H₂/19% He/1% CH₄, would be free-piston driven to reduce possible contamination from an arc driver, utilise pure hydrogen as the driver gas, and feature a disposable shock tube to minimise carbon contamination. Although many of these things are very difficult to implement, it would be interesting to explore if data obtained in T6 could contribute to validation of this model.

5.2. Performance Envelope Expansion

The use of Stalker substitution to expand the operating envelope of ground test facilities has been investigated in detail at the University of Queensland [20]. This technique presents an exciting opportunity to reach higher and higher shock speeds, however the science of exactly how such scaled test conditions can be related to flight, particularly where radiative heat flux is concerned, would

benefit from further study. T6 is uniquely positioned, because of its multi-modal design, to make direct comparisons between radiative spectra in shock tube mode and Stalker substituted conditions in expansion tube mode and provide insight into the underlying physics at play.

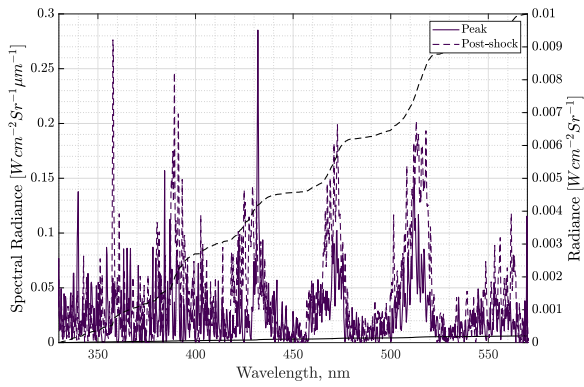
As discussed in the accompanying paper on Ice Giant expansion tunnel experiments in T6 there are other options to improve the facility performance including the use of thinner secondary diaphragm material and the design of new driver conditions which would include a new piston, diaphragm, or orifice plate removal. An alternative method is the design of another steel tertiary barrel with a smaller internal diameter. This would offer a relatively minimal performance increment, though [21].

6. CONCLUSION

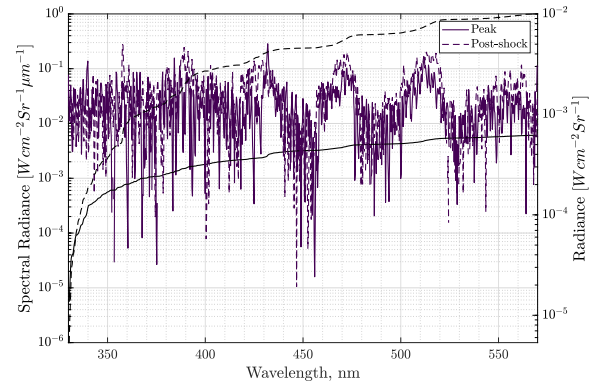
The development and demonstration of a new Ice Giant entry simulation capability in T6 and Europe has been presented. Measurements of shock-layer radiation were obtained via emission spectroscopy for H/He mixtures including CH₄. The presence of CH₄ appears to strongly affect the spectral radiance in the post-shock region, particularly via the Deslandres-D'Azambuja band system of C2, which has direct implications for mission planning to Neptune and Saturn.

ACKNOWLEDGMENTS

This work is funded within an ESA initiative under contract No. 4000132571/20/NL/MG/rk. We thank the colleagues of the research team in Stuttgart and Oxford. We would also like to acknowledge the building services and workshop staff at the Southwell Building, Millbrook Precision Ltd.

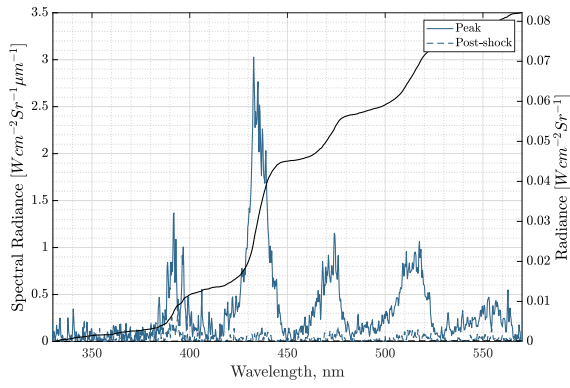


(a) Linear scale

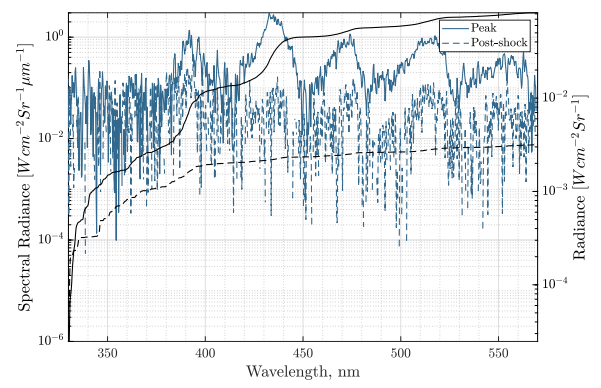


(b) Log scale

Figure 7: Spectral radiance versus wavelength for the 0% methane condition

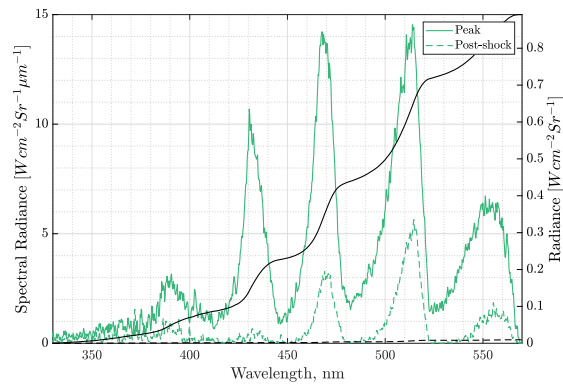


(a) Linear scale

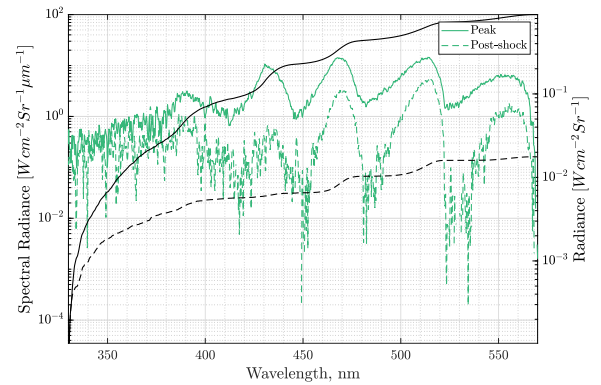


(b) Log scale

Figure 8: Spectral radiance versus wavelength for the 0.5% methane condition



(a) Linear scale



(b) Log scale

Figure 9: Spectral radiance versus wavelength for the 5% methane condition

REFERENCES

- [1] Committee on the Planetary Science and Astrobiology Decadal Survey, Space Studies Board, Division on Engineering and Physical Sciences, and National Academies of Sciences, Engineering, and Medicine. *Origins, Worlds, and Life: A Decadal Strategy for Planetary Science and Astrobiology 2023-2032*. 2022.
- [2] S Bayon. CDF Study Report - Ice Giants. page 431, 2019.
- [3] Mark Hofstadter, Amy Simon, Sushil Atreya, Donald Banfield, Jonathan J. Fortney, Alexander Hayes, Matthew Hedman, George Hospodarsky, Kathleen Mandt, Adam Masters, Mark Showalter, Krista M. Soderlund, Diego Turrini, Elizabeth Turtle, Kim Reh, John Elliott, Nitin Arora, and Anastassios Petropoulos. Uranus and Neptune missions: A study in advance of the next Planetary Science Decadal Survey. *Planetary and Space Science*, 177:104680, November 2019.
- [4] Grant Palmer, Dinesh Prabhu, and Brett A. Cruden. Aeroheating Uncertainties in Uranus and Saturn Entries by the Monte Carlo Method. *Journal of Spacecraft and Rockets*, 51(3):801–814, May 2014.
- [5] Brett A. Cruden and David W. Bogdanoff. Shock Radiation Tests for Saturn and Uranus Entry Probes. *Journal of Spacecraft and Rockets*, 54(6):1246–1257, November 2017.
- [6] J. I. Moses, T. Cavalié, L. N. Fletcher, and M. T. Roman. Atmospheric chemistry on Uranus and Neptune. *Philosophical Transactions of the Royal Society A: Mathematical, Physical and Engineering Sciences*, 378(2187):20190477, December 2020.
- [7] João Alexandre Abreu Coelho. Aerothermodynamic Analysis of Aerocapture and Ballistic Entry Flows in Neptune’s Atmosphere. page 134, 2021.
- [8] A. M. Brandis, D. A. Saunders, C. O. Johnston, B. A. Cruden, and T. R. White. Radiative Heating on the After-Body of Martian Entry Vehicles. *Journal of Thermophysics and Heat Transfer*, 34(1):66–77, January 2020.
- [9] Peter Collen, Luke J Doherty, D Subiah, Tamara Sopek, David Gildfind, Rowland Penty, Rowan Gollan, and Richard Morgan. Development and Commissioning of the T6 Stalker Tunnel. page 41, 2021.
- [10] Matthew McGilvray, Peter Collen, Luke Doherty, Joseph Steer, James Leader, Alex Glenn, and Chris Hambidge. The Oxford T6 Stalker tunnel: performance, upgrades and new modes of operation. In *FAR Conference*, 2022.
- [11] PL Collen. *Development of a high-enthalpy ground test facility for shock-layer radiation*. PhD thesis, Ph. D. thesis. University of Oxford, 2021.
- [12] Alex B. Glenn, Peter L. Collen, and Matthew McGilvray. Experimental Non-Equilibrium Radiation Measurements for Low-Earth Orbit Return. In *AIAA SCITECH 2022 Forum*, San Diego, CA & Virtual, January 2022. American Institute of Aeronautics and Astronautics.
- [13] Christopher James. *Radiation from simulated atmospheric entry into the gas giants*. PhD Thesis, The University of Queensland, October 2018.
- [14] Chul Park. Stagnation-point radiative heat fluxes in Neptune aerocapture. In *Seventh international planetary probe workshop, barcelona*, pages 14–18, 2010.
- [15] Chul Park. Nonequilibrium Ionization and Radiation in Hydrogen-Helium Mixtures. *Journal of Thermophysics and Heat Transfer*, 26(2):231–243, April 2012.
- [16] Floyd R. Livingston and P. T. Y. Poon. Relaxation Distance and Equilibrium Electron Density Measurements in Hydrogen-Helium Plasmas. *AIAA Journal*, 14(9):1335–1337, September 1976.
- [17] Lewis P. Leibowitz. Measurements of the structure of an ionizing shock wave in a hydrogen-helium mixture. *Physics of Fluids*, 16(1):59, 1973.
- [18] Chul Park. Nonequilibrium Chemistry and Radiation for Neptune Entry. *Journal of Spacecraft and Rockets*, 48(6):897–903, November 2011.
- [19] C. Park. Reactions in H₂+He+CH₄ in Strong Shock Waves: A Review. In Konstantinos Kontis, editor, *28th International Symposium on Shock Waves*, pages 139–144. Springer Berlin Heidelberg, Berlin, Heidelberg, 2012.
- [20] Yu Liu, Christopher M. James, Richard G. Morgan, and Timothy J. McIntyre. Experimental validation of a test gas substitution for simulating non-equilibrium giant planet entry conditions in impulse facilities. *Experiments in Fluids*, 61(9):198, September 2020.
- [21] George Emanuel, U. S. Satyanand, and Frank K. Lu. Performance of a Shock Tube with a Large-Area Contraction. *AIAA Journal*, 43(9):1995–1999, September 2005.